Eleuterochori

Archaeological Background

On the same hill, where the school of the modern village of Eleftherochi is located, there is also a Neolithic settlement. Generally it is placed at the north side of the natural passage from the plain of Almyros to the Farsala and the west Thessaly plain, on a hilly terrain quite different from that of the flat Thessalian plains.

The only information about this settlement is a short reference to its existence as a result of an extensive survey conducted by the 13th Ephorate of Prehistoric and Classical Antiquities and the Italian Archaeological School at Athens (in the 1980s).

Geophysical Prospection

Electromagnetic Induction Survey

EM survey was conducted with the GEM2 from Geophex using 5 frequencies. We did a profile every 1 m with a grid positioning. Data acquisition was done in the schoolyard as in the other method. The bad calibration procedure did not allow for a conversion in electrical conductivity and magnetic susceptibility. We are then speaking only in term of quadrature and the in-phase part of the EM signal. Both of these are closely related to the electrical conductivity and the magnetic susceptibility.

The quadrature out-of-phase part of the signal shows some effects induced by the fence delimiting the schoolyard and the main building (Figure 1). The effects of modern intrusion are clearly visible on the border (and corner) of the map. In the south, the EM shows a large conductive anomaly. The origin of this anomaly could be archaeological, even if it is not visible in other data (such as GPR). Otherwise, some small anomalies are probably induced by trees and recent disturbance. The in-phase part of the signal does not show any clear anomalies (Figure 2). Only disturbances close to the fence and the main building are visible. In the east part of the map, the data clearly show the presence of a pipe.

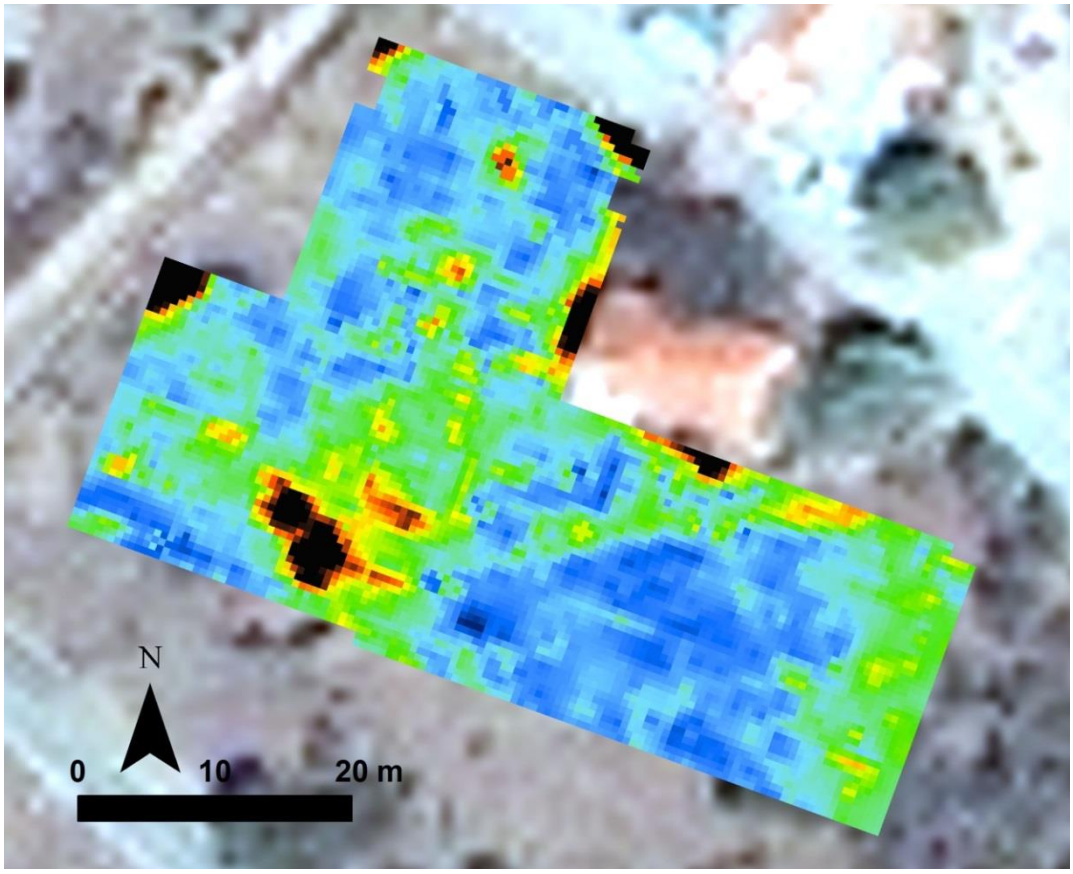

Figure 1: Quadrature part of the GEM2 measurement

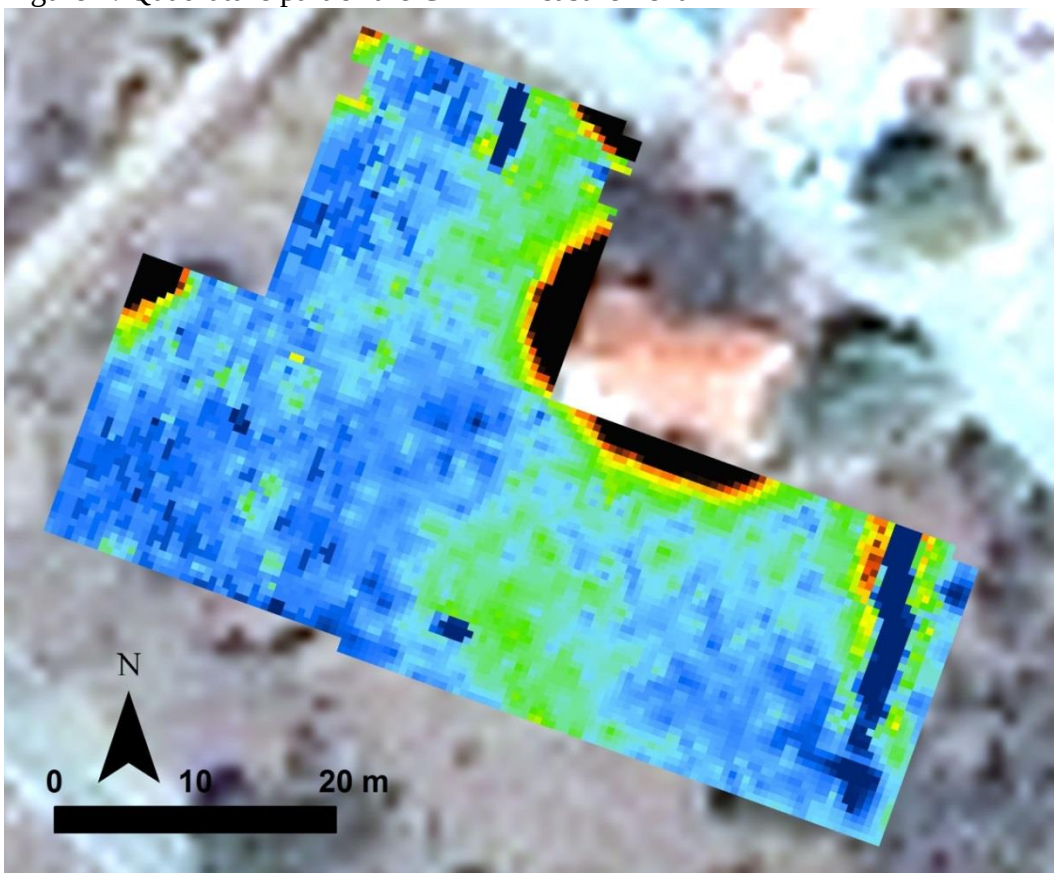

Figure 2: In-phase of the GEM2 measurement

Ground Penetrating Radar Survey

The survey with the Noggin Plus smart cart was conducted inside the schoolyard. The area covered is 2180 m^2 and consists of 6 grids. The resulting slices are presented in Table 1. The filters and corrections that are applied in this case are: Trace Reposition, Repick first break (15%), Dewow, Sec2 (Atn=9.29 dB_m, StrtG=5.9, MaxG=709), Background Average Subtraction, Bandpass filter (Fc1=40 % Freq, Fp1=80 % Freq, Fp2=160 % Freq, Fc2=200 % Freq), Lowpass filter (f=30 % Nyquist), Bandpass filter (Fc1=40 % Freq,Fp1=80 % Freq,Fp2=120 % Freq,Fc2=160 % Freq), Background Average Subtraction.

Overall, the results exhibit some strong anomalies of irregular shape. The ones identified within the range of 0-40 cm from the surface are most likely to be caused by debris and remains of recent construction. The most important anomalies which appeared in the results are also shown in Figure 3.

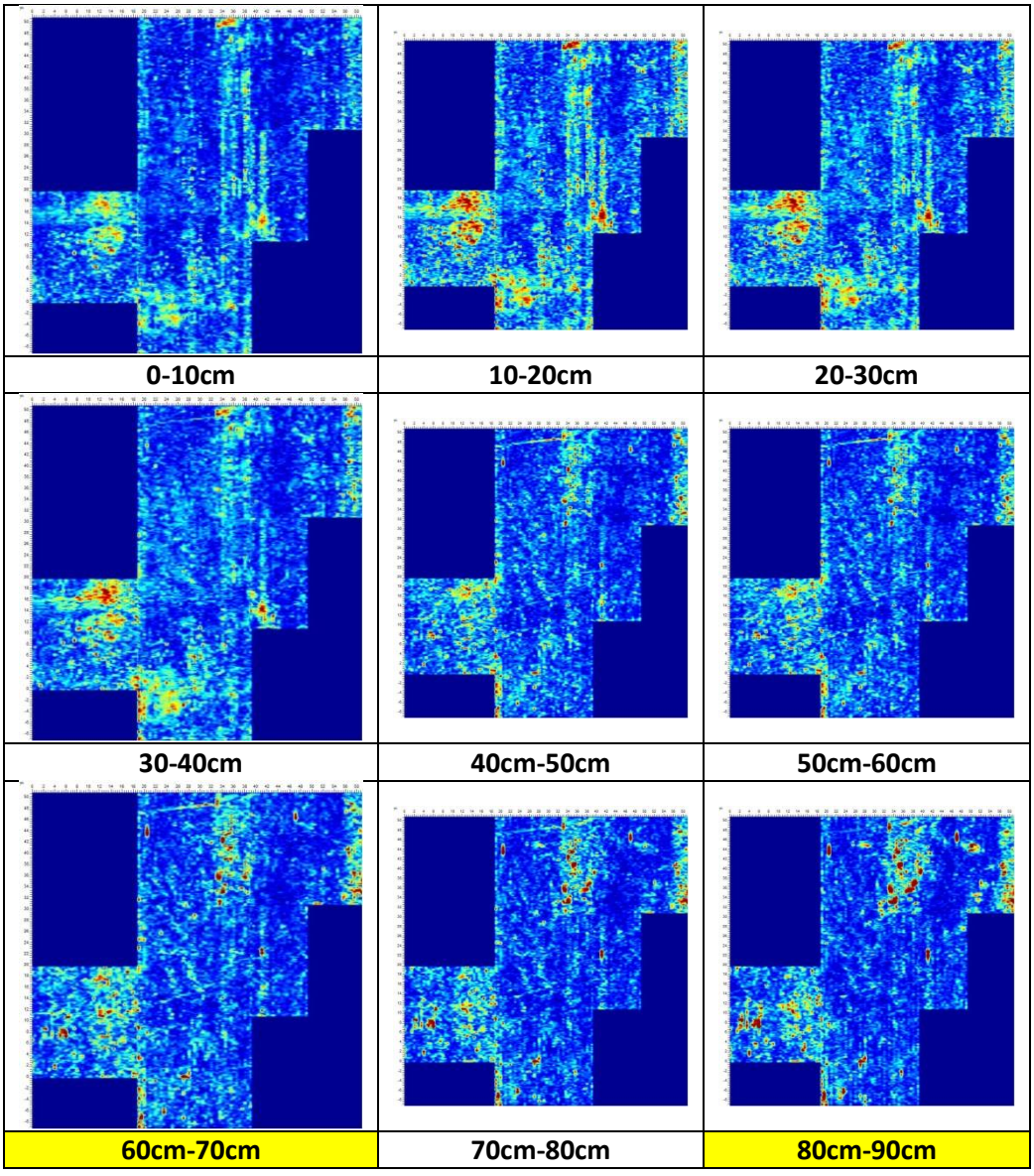

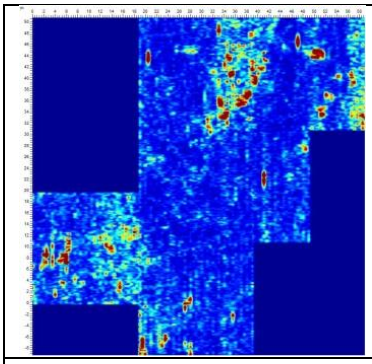	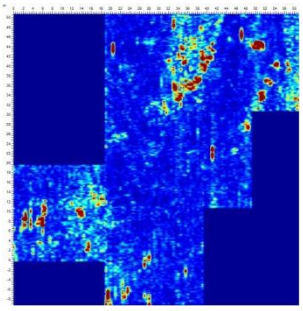	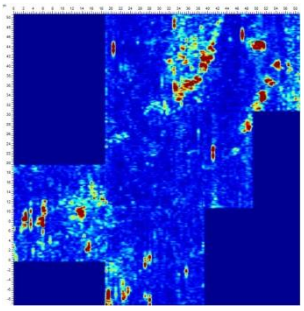
90cm-100cm	100cm-110cm	110cm-120cm
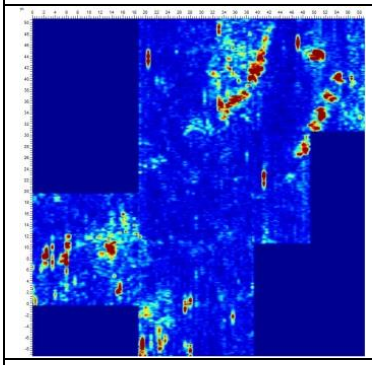	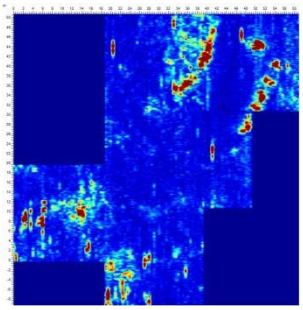	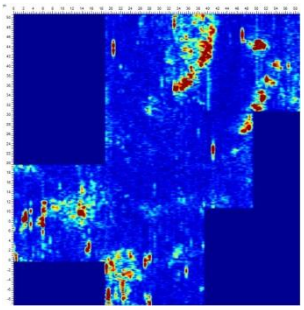
120cm-130cm	130cm-140cm	140cm-150cm
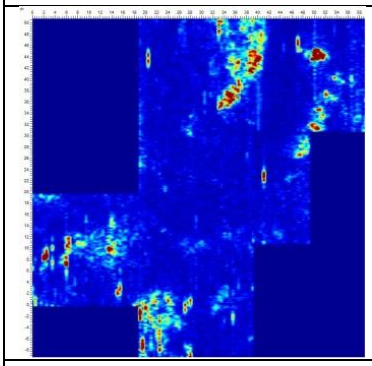	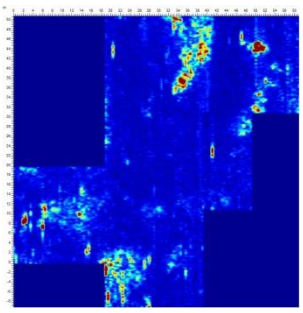	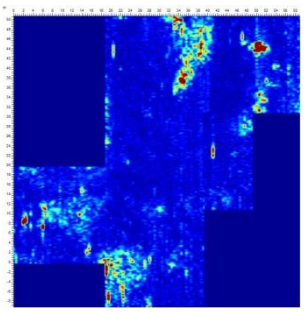
150cm-160cm	160cm-170cm	170cm-180cm
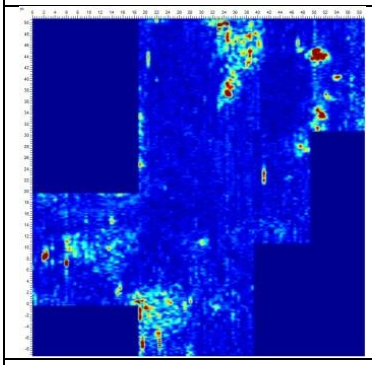	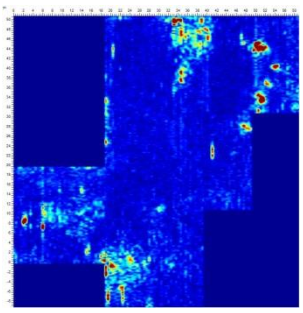	
180cm-190cm	190cm-200cm	

Table 1: GPR depth slices for the grids with code names EL1 to EL6 at Eleutherochori with 10 cm thickness.

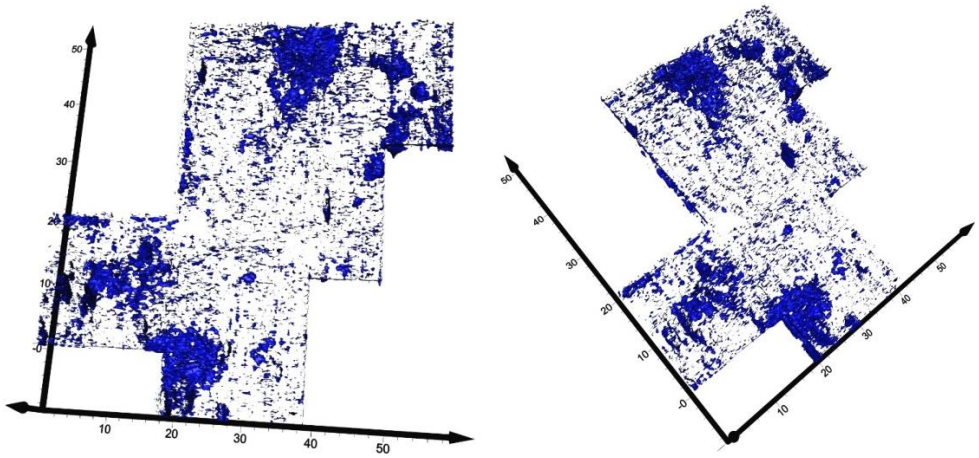

Figure 3: Different perspectives of the GPR 3D model describing the subsurface from the surface and up to 2.0 m depth.

In Figure 4, georeferenced GPR slices within the range of 50-100 cm are presented with their corresponding interpretation. The images have been superimposed on an aerial photograph of the area. The linear anomaly A1 (Figures 4a and 4b) that first shows up at 40 cm depth and extends up to 80 cm is assigned to a water pipe. At 80-90 cm depth (Figure 4c) a group of three strong anomalies described by A2 in Figure 2d are visible. Those anomalies present linearity and are parallel to each other. A2 exhibits strong amplitudes up to 150 cm.

The strongest amplitudes in this case appear deeper than 100 cm (Figure 5). The anomaly A3 (Figure 5b) describes a group of strong amplitudes that define two areas of irregular shape. The anomaly A4 describes a large wedge-shaped area that exhibits the strongest amplitudes. It first appears at 60 cm, but its shape becomes clearer within the range of 100-150 cm. At 140-150 cm, a strong linear reflector (Figures 3c and 3d) becomes visible and is oriented northwest-southeast. The reflector A4 is positioned within trees, and due to its geometry could be assigned to a geological feature. The circular anomaly A5 (Figure 5d) appears at 100 cm and seems to extend below 200 cm. Similar reflectors to A5 are those described by A6, which appear from 100-150 cm from the surface. They also present a linearity of similar orientation to A4. Last, the anomaly A7 appears at 140-150 cm depth (Figures 5b and 5d). It exhibits weaker amplitudes compared to the rest of the anomalies described before and defines a circular area.

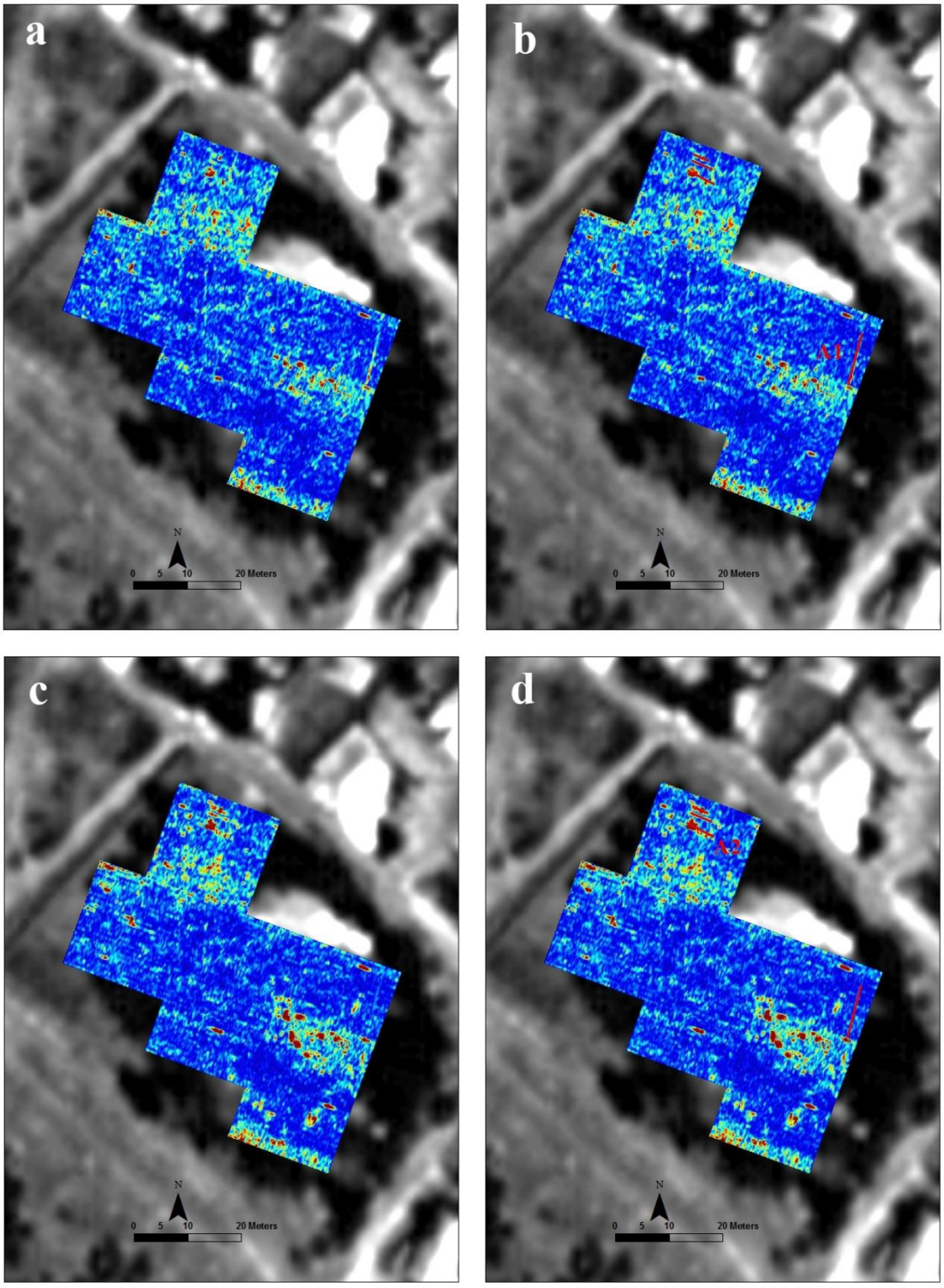

Figure 4: GPR results within the range 50-100 cm. a) The georeferenced slice for 60-70 cm depth, b) the most important anomalies for 60-70 cm depth, c) the georeferenced slice for 80-90 cm depth, and d) the anomalies for 80-90 cm depth.

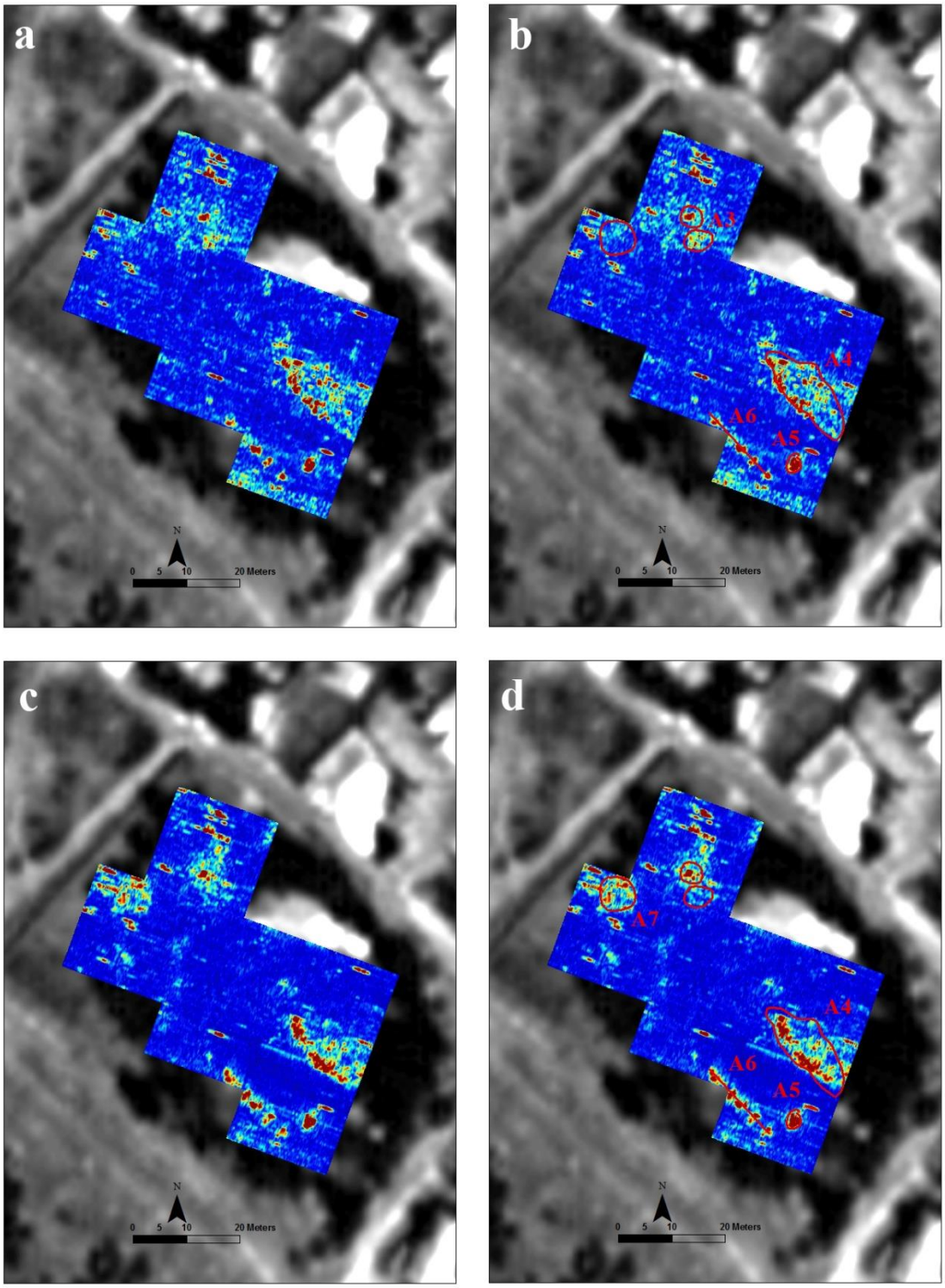

Figure 5: GPR results below 100 cm depth. a) The georeferenced slice for 100-110 cm depth, b) the most important anomalies for 100-110 cm depth, c) the georeferenced slice for 140-150 cm depth, and d) the anomalies for 140-150 cm depth.

Resistance Survey

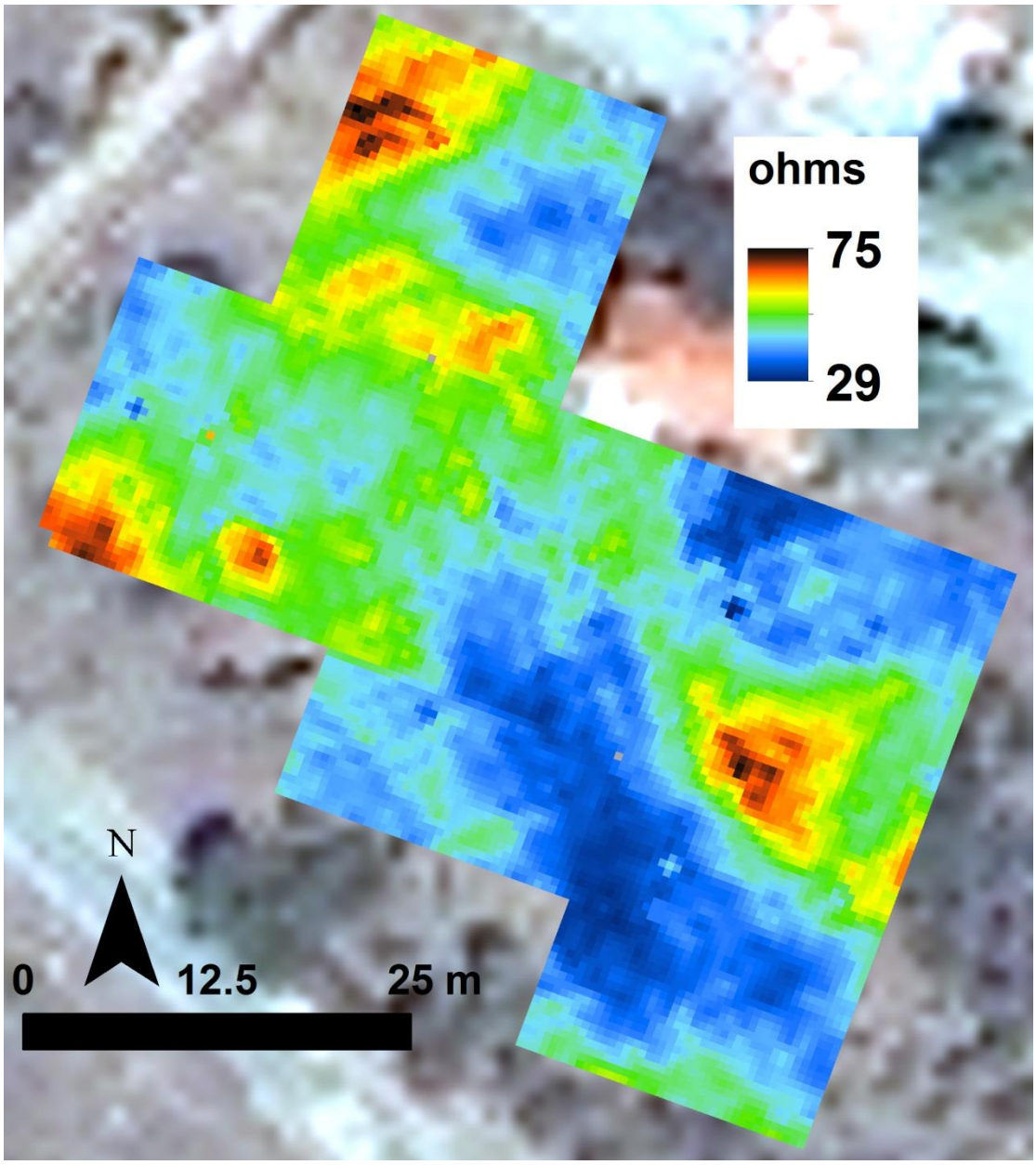

Figure 6: Distribution of resistance anomalies at Eleuterochori

Results of the resistance survey at Eleuterochori reveal concentrations of high-resistance anomalies at three locations and two low-resistance zones. The northernmost high-resistance anomaly is oriented in a northeast-southwest direction, but cut short in the west by the survey coverage. Another high-resistance anomaly is located at the westernmost corner of the study area. There again, the boundaries of the actual anomaly cannot be determined due to coverage. The eastern anomaly, however, is spatially well defined. Moreover, it matches with the GPR anomaly A4. Curiously, another GPR anomaly, A7, does not provide the same signature and hint of differential physical structures of subsurface features.

Two low-resistance anomalies appear as contiguous surfaces. The northern zone follows a northeast-southwest direction, and the southern zone follows a southeast-northwest direction—overall creating a triangular shape and enveloping the

easternmost high-resistance anomaly. The northern low-resistance anomaly is cut off by the survey coverage, and its extent in the northeast remains undetermined. The southern low-resistance anomaly is also located between the GPR anomalies: A4, A5, and A6.

Vertical Electric Sounding

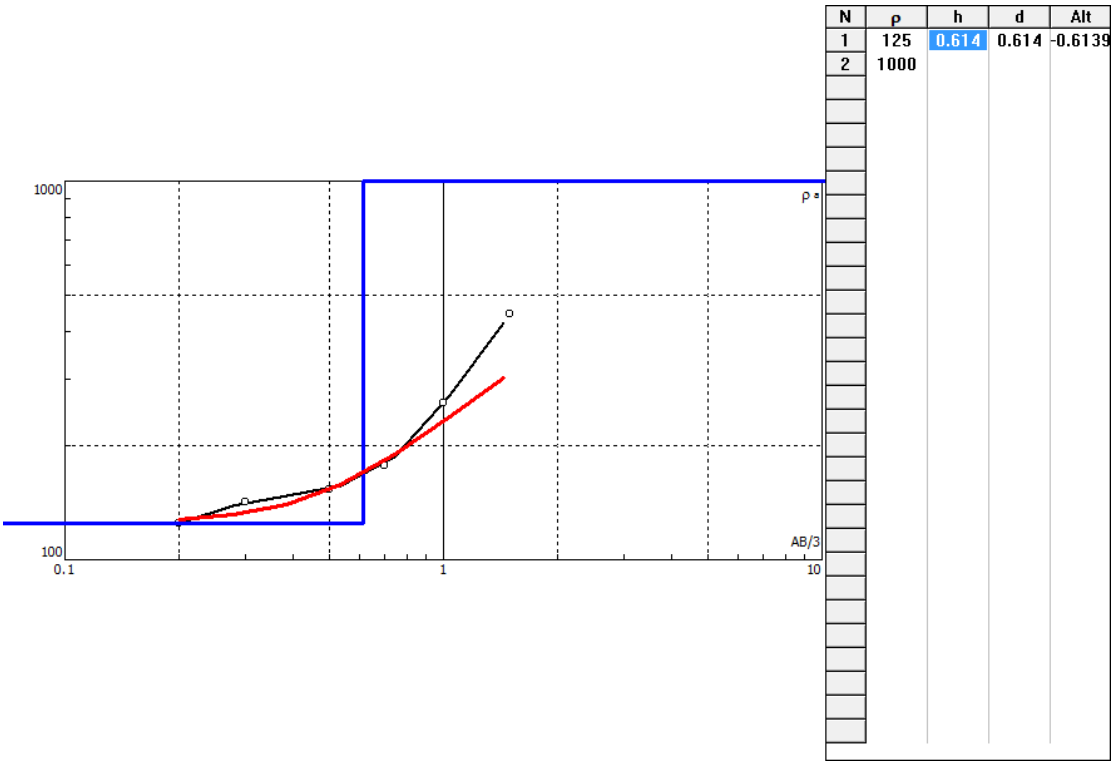

Figure 7: Inversion results of the VES measurement done on the center of the schoolyard in front of the school building.

Site Bibliography

Ιντζεσίλογλου Α., 1995. *Επιφανειακές έρευνες, Νομός Μαγνησίας*, *ΑΔ* 44 (1989), *Χρονικά*, 228-229